Charge state switching of Cu acceptors in ZnO nanorods

M. Azizar Rahman,[1] Mika T. Westerhausen,[1] Christian Nenstiel,[2] Sumin Choi,[1] Axel Hoffmann,[2] Angus Gentle,[1] Matthew R. Phillips,[1] and Cuong Ton-That[1,a)]
[1]*School of Mathematical and Physical Sciences, University of Technology Sydney, PO Box 123, NSW 2007, Australia*
[2]*Institut für Festkörperphysik, Technische Universität Berlin, Hardenbergstr. 36 10623 Berlin, Germany*

(Received 24 December 2016; accepted 6 March 2017; published online 21 March 2017)

Undoped and Ga-doped ZnO nanorods both exhibit an intense green luminescence (GL) band centered at ~2.4 eV. Unlike the defect-related GL in undoped nanorods, the GL band in Ga-doped nanorods displays a periodic fine structure separated by 72 meV, which consists of doublets with an energy spacing of 30 ± 3 meV. The emergence of the structured GL is due to the Cu^+ state being stabilized by the rise in the Fermi level above the 0/- (Cu^{2+}/Cu^+) charge transfer level as a result of Ga donor incorporation. From a combination of optical characterization and simulation using the Brownian oscillator model, the doublet fine structures are shown to originate from two hole transitions with the Cu^+ state located at 390 meV above the valence band. *Published by AIP Publishing.* [http://dx.doi.org/10.1063/1.4978761]

The optoelectronic properties of ZnO can be enhanced and tailored by doping it with Ga, opening up possible applications, such as tunable plasmonic devices and optically transparent electrodes in dye-sensitized solar cells.[1,2] First principle calculations and experiments have shown that Ga favorably occupies substitutionally the Zn site (Ga_{Zn}), which acts as a shallow donor leading to the formation of Ga-bound excitons that produce sharp luminescence lines at low temperature known as I_1 and I_8 lines.[3,4] However, there have been few studies to date that investigate the effect of Ga doping on the ubiquitous broad visible emission in ZnO. This deep-level emission in ZnO is most commonly observed in the green and widely accepted to be associated with intrinsic defects (such as oxygen and zinc vacancies) or the internal transition of a hole within substitutional Cu_{Zn} centers.[5,6]

Cu is a commonly incorporated impurity up to the ppm level in II–VI semiconductors such as ZnS, ZnO, and CdS and is known to form acceptor states within the bandgap. A large amount of work on Cu-doped ZnO exists concerning various aspects of its acceptor states and their possible role in green luminescence mechanism.[7–9] Cu dopants have also been theoretically predicted to favor spin polarization and hole mediated ferromagnetism in ZnO-based diluted magnetic semiconductors.[10] Room temperature ferromagnetism of Cu-doped ZnO has been reported by different groups;[11,12] conversely, the lack of ferromagnetism in some samples was also confirmed by other workers.[13] These inconsistent results highlight the fact that the nature of Cu acceptors in ZnO and its role in the optical and magnetic properties is highly controversial. In this work, we demonstrate that the charge state of Cu in ZnO nanorods can be selectively switched by Ga doping. This switching behavior of the Cu charge state could account for the often contradictory interpretations of the luminescence and ferromagnetism properties of Cu-doped ZnO. To elucidate and predict the carrier mediated conversion of the Cu charge state in ZnO we have performed optical measurements and simulation of the characteristic Cu-related green luminescence (GL) band in ZnO nanorods fabricated the vapor-liquid-solid (VLS) method. This growth method enables the manipulation of the electronic structure of ZnO nanorods by uniformly introducing Ga dopants substitutionally on Zn sites during the growth. The spectral simulation of the Cu-related GL enables the determination of the zero phonon line (ZPL) and phonon coupling strength of the Cu luminescence center in ZnO.

ZnO nanorods were grown on highly polished silicon (100) wafers and quartz substrates by the VLS method described in detail elsewhere.[14] To grow Ga-doped ZnO nanorods, Ga_2O_3 powder (Sigma Aldrich, 99.99% pure) was added to the source material. The morphological and elemental analyses were performed using Zeiss Supra 55VP scanning electron microscope (SEM) attached with an Energy Dispersive X-ray (EDX) spectrometer for qualitative elemental mapping. The Ga and Cu concentrations in the nanorods were analyzed by Laser Ablation (Teledyne Cetac LSX-266) Inductively Coupled Plasma Mass Spectrometry (Agilent 7500cx). Photoluminescence (PL) measurements were performed using the 325 nm emission line of a HeCd laser and the emitted light was dispersed by a Spex-1404 double monochromator (spectral resolution 50 μeV). Cathodoluminescence (CL) was performed using a FEI Quanta 200 SEM equipped with a high-resolution Hamamatsu S7011–1007 CCD image sensor.

Fig. 1(a) shows a secondary electron SEM image of Ga-doped ZnO nanorods containing 0.15 ± 0.06 at % Ga. Nearly all the nanorods are aligned along the [0002] direction perpendicular to the substrate (see the X-ray diffraction patterns in Fig. S1 in supplementary material) and possess hexagonal tip facets, indicating that the nanorods are single crystal wurtzite. The nanorods typically have diameters of ~130 nm and lengths of ~450 nm. EDX elemental mapping was used to qualitatively evaluate the spatial uniformity of distributions of Ga and Zn in the nanorods. The EDX maps in Fig. 1(b) show uniform distribution of Ga and Zn along the Ga-doped ZnO nanorods. The LA-ICP-MS analysis reveals a Cu

a)Author to whom correspondence should be addressed. Electronic mail:Cuong.Ton-That@uts.edu.au

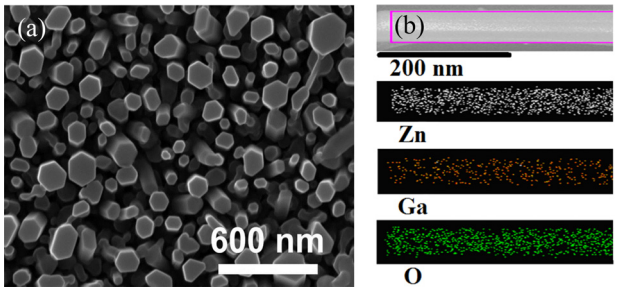

FIG. 1. (a) A typical secondary electron SEM image of 0.15% Ga-doped ZnO nanorods showing vertically aligned nanorods with hexagonal well-faceted cross-section (b) SEM image of an isolated NW which has been extracted from the substrate and its corresponding EDX elemental maps showing a generally uniform spatial distribution of Ga along the nanowire length.

concentration of ~30 ppm in both undoped and Ga-doped nanorods using the NIST 610 and 612 standard reference materials.

The near-band-edge (NBE) PL spectra of the ZnO nanorods show free exciton (FX) and bound exciton (D^oX) emissions at 3.381 and 3.365 eV, respectively, together with their corresponding longitudinal optical (LO) phonon replicas [Fig. 2(a)]. The inset shows high-resolution PL spectra with well-resolved bound exciton lines I_4 (due to H impurities) and I_6 (due to Al).[3] For the Ga-doped nanorods, the NBE emission is dominated by the I_8 line at 3.364 eV attributed to excitons bound to neutral Ga donors,[4] while I_1 has been assigned to ionized-Ga donor bound excitons.[15] These well-resolved free and bound excitonic lines suggest that the Ga-doped nanorods remain non-degenerate. Additionally, the strong I_8 line indicates that Ga dopant atoms are incorporated in the nanorods by predominantly substituting Zn. The deep-level PL spectra of the undoped and Ga-doped ZnO nanorods at 6 K are depicted in Fig. 2(b). Comparison of the nanorods PL spectra before and after the Ga doping reveals the following: (i) the fine structured doublets emerges, with an energy spacing equal to the longitudinal optical phonon energy $E_{LO} = 72 \pm 3$ meV, and (ii) the GL peak is red shifted by ~50 meV. The symmetrical, unstructured GL band centered at 2.45 eV in undoped ZnO is attributable to zinc vacancies (V_{Zn}) in earlier work.[5,16] It is noteworthy that the optical quality of the nanorods improves significantly upon the Ga doping as Ga atoms occupies V_{Zn} sites in the as-grown nanorods as evidenced by the increase in the E_2^{high} mode in Raman spectra (see the Raman spectra in Fig. S3, supplementary material). The Ga-doped ZnO nanorods exhibit a sharp ZPL peak at 2.874 eV and a series of doublets whose energy positions match, within the experimental error of ±20 meV, those reported in the literature for bulk Cu-doped ZnO[17] (see Table S1 in supplementary material), indicating that the Ga doping activates Cu luminescence centers. The slight variations in the exact peak positions could also be due to tensile strain in the ZnO nanorods.[18]

The most plausible explanation for the activation of Cu luminescence centers is the conversion of the Cu acceptor charge state from Cu^{2+} to Cu^{+} as the Fermi level is raised above the 0/- (Cu^{2+}/Cu^{+}) charge transfer level (located at 180 meV below the conduction band minimum).[19] In the Ga-doped ZnO nanorods, the activated Cu^{+} centers provide

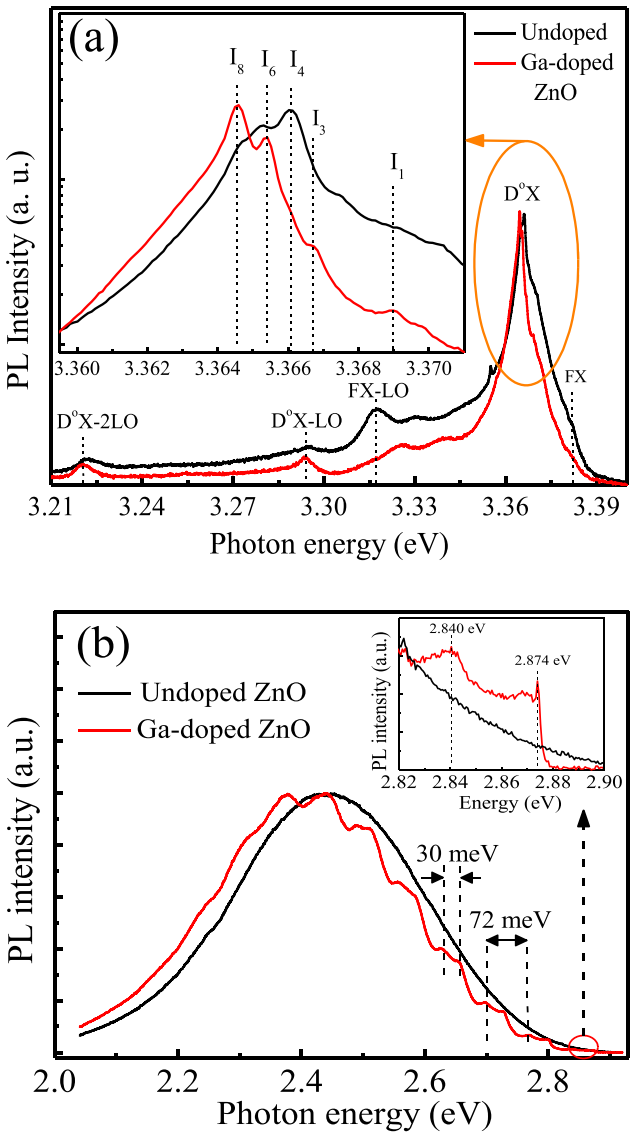

FIG. 2. (a) Near band edge PL emission spectra of the undoped and Ga-doped ZnO nanorods at 6 K showing Ga donor bound exciton lines I_1 and I_8. (b) Deep level emission of PL spectra for the nanorods. The doublet fine structures with 72 ± 3 meV periodicity emerge after the Ga doping. The spacing of the doublet features is 30 ± 3 meV. The inset shows the sharp zero phonon lines at 2.874 and 2.840 eV.

the dominant recombination pathway, while the V_{Zn}-related GL emission is quenched as a result of Ga occupation at V_{Zn} sites. It is worth noting that the carrier concentration in these ZnO nanorods is several orders of magnitude lower than that in degenerate Ga-doped ZnO films ($n > 10^{20}$ cm^{-3});[20] thus, the self-compensation effect by lowering the formation energy of V_{Zn} would be less pronounced in this case. For non-degenerate ZnO nanorods, which are large enough to avoid quantum size effects, the carrier concentration can be estimated by[21]

$$n \approx 2(m_e kT/2\pi\hbar^2)^{3/2} \exp\left[(E_f - E_c)/kT\right], \qquad (1)$$

where m_e is the electron effective mass, and E_f and E_c are the Fermi energy and conduction band minimum, respectively. The other symbols have their usual meaning. In order to activate the Cu^{+} luminescence center, the Fermi level must rise above the $Cu^{2+}(A^o)/Cu^{+}(A^-)$ (0/-) charge transfer level

(CTL). The Fermi level shift due to the Ga doping is confirmed by valence-band X-ray photoemission spectroscopy, which reveals that the energetic gap ($E_V - E_F$) between the valence band maximum and Fermi level is 3.05 and 3.24 eV for the undoped and Ga-doped nanorods, respectively (Fig. S4(a), supplementary material). Since the bandgap is the same for the undoped and Ga-doped nanorods (Fig. S4(b), supplementary material), the increase in the ($E_V - E_F$) gap indicates that the Fermi level is raised towards the conduction band after the Ga doping. Considering the optical bandgap of 3.29 eV, this result suggests flat bands or slight upward band bending in the near-surface region.[22] Knowing the position of the Fermi level and $m_e = 0.29m_o$ (m_o is the rest mass),[23] the carrier concentration can be estimated using equation (1), which yields $n \approx 6.2 \times 10^{17}$ cm^{-3} for the Ga-doped nanorods at 300 K. This estimated electron concentration in the Ga-doped nanorods is significantly lower than the value expected for ZnO doped with 0.15% Ga, likely because of formation of acceptor-like defects as a result of self-compensation.[20] Additionally, a significant proportion of Ga donors could be in the neutral state, as evidenced by the fact that the PL spectrum of the Ga-doped nanorods at 6 K (Fig 2(a)) is dominated by the neutral-Ga donor bound I_8 rather than ionized-Ga donor bound I_1. This result provides a physical picture of the structured GL in the Ga-doped nanorods: the Cu^+ state is stabilized by the rise in the Fermi level and can readily trap free holes from neighboring oxygen atoms by the potential created by the additional electron in the ionized acceptor $Cu^+(3d^{10})$ state,[24] which gives rise to the structured GL. The doublets in the Cu-related structured GL (with an energy spacing of 30 ± 2 meV, see Table S1, supplementary material) are due to the two kinds of energetically different holes that are transferred from the orbitals surrounding the oxygen atom to the 3*d* shell of copper.[17] The change in the chemical origin of the GL from V_{Zn} to Cu centers also accounts for the observed red shift in the GL after the Ga doping. Further support for these attributions comes from the temperature dependence of the energetic positions for the structured and structureless GL bands (Fig. S3, supplementary material). The ZPLs and their phonon replicas of the structured GL remain unchanged in position with increasing temperature, characteristic of an internal transition within Cu centers.

To investigate the nature of the Cu luminescence centres responsible for the structured GL, the emission band was simulated using multimode Brownian oscillator (MBO) model,[25] in which the electronic transitions between the Cu ground and excited states was examined. The variables used in the MBO model are the Huang–Rhys factor (S) that reflects the phonon coupling strength and the coefficient (γ_j) that reflects the full width at half maxima of the LO-phonon side band. At $T \rightarrow 0$, the PL intensity according to the MBO model can be expressed as[25]

$$I_{PL}(\omega) = \sum_{n=0}^{\infty} \frac{S^n \exp(-S)}{n!} \times \frac{(\gamma_{ZPL} + n\gamma_j)/2\pi}{(\hbar\omega - \hbar\omega_{eg} + n\hbar\omega_{LO}) + (\gamma_{ZPL} + n\gamma_j)/2}, \quad (2)$$

where γ_{ZPL} is the width of the ZPL, n the number of phonons, $\hbar\omega$ the energy of the emission band, and $\hbar\omega_{eg}$ the separation energy between the ground and excited states. To simulate the GL spectra, we adopted a simplified MBO model in which only the LO phonon oscillator ($\hbar\omega_{LO} = 72\,meV$) was considered. The simulated spectra, displayed as solid curves in Fig. 3, demonstrate the best fits with the following parameters: (i) $\hbar\omega_{eg1} = 2874\,meV$, $\hbar\omega_{eg2} = 2844\,meV$, $\gamma_j = 7.4 \pm 0.3\,meV$, and $S = 6.55 \pm 0.04$ for the Ga-doped ZnO nanorods; and (ii) $\hbar\omega_{eg} = 2910\,meV$, $\gamma_j = 8.7 \pm 0.3\,meV$, and $S = 6.75 \pm 0.04$ for the structureless ZnO GL. The simulated $\hbar\omega_{eg1}$ and $\hbar\omega_{eg2}$ values are consistent with the energetic positions of the ZPLs for the Ga-doped nanorods shown in Table S1 (supplementary material). The Huang–Rhys factor of 6.55 for the Ga-doped ZnO GL is consistent with the literature value of Cu-doped ZnO.[26] Taking the ground state energy of Cu^{2+} at 180 meV below the conduction band maximum,[9] the activation energy of the excited state (Cu^+, *h*) state in the Ga-doped ZnO nanorods can be determined to be 390 meV from the simulated $\hbar\omega_{eg}$ values. Fig. 4 depicts the electronic transitions involved in the Cu ground and excited states of the Ga-doped ZnO nanorods. With the Fermi level raised by the Ga doping, Cu is in its Cu^+ state and acts as negatively charged ionized acceptor. This Cu^+ state captures holes from the neighboring oxygen, placing it in an excited state (Cu^+, h), and the hole is then transferred to the 3*d* shell to form Cu^{2+} ($3d^9$). This charge transfer results in the structured GL emission in the Ga-doped ZnO nanorods.

In conclusion, we report the carrier-mediated switching behavior of Cu acceptors in ZnO nanorods by Ga doping. Using the vapor-liquid-solid growth, Ga is *in-situ* incorporated substitutionally at Zn lattice sites in nanorods without compromising the crystal quality, producing Ga donor-bound exciton signatures in ZnO. The Ga donor doping increases the carrier density which pushes the Fermi-level above the $Cu^{+/2+}$ charge transfer level, producing doublet

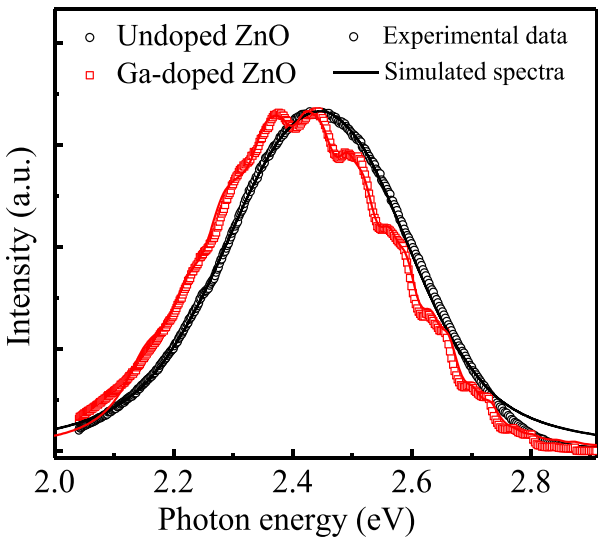

FIG. 3. Theoretically generated GL bands (solid curves) for the undoped and Ga-doped ZnO nanorods using the MBO model. The open circles represent the measured spectra at 6 K. The best fit to the doublet fine structures in the Ga-doped nanorods is obtained using Eq. (2) with $\hbar\omega_{eg1} = 2874$ meV, $\hbar\omega_{eg2} = 2844$ meV, and $S = 6.55$.

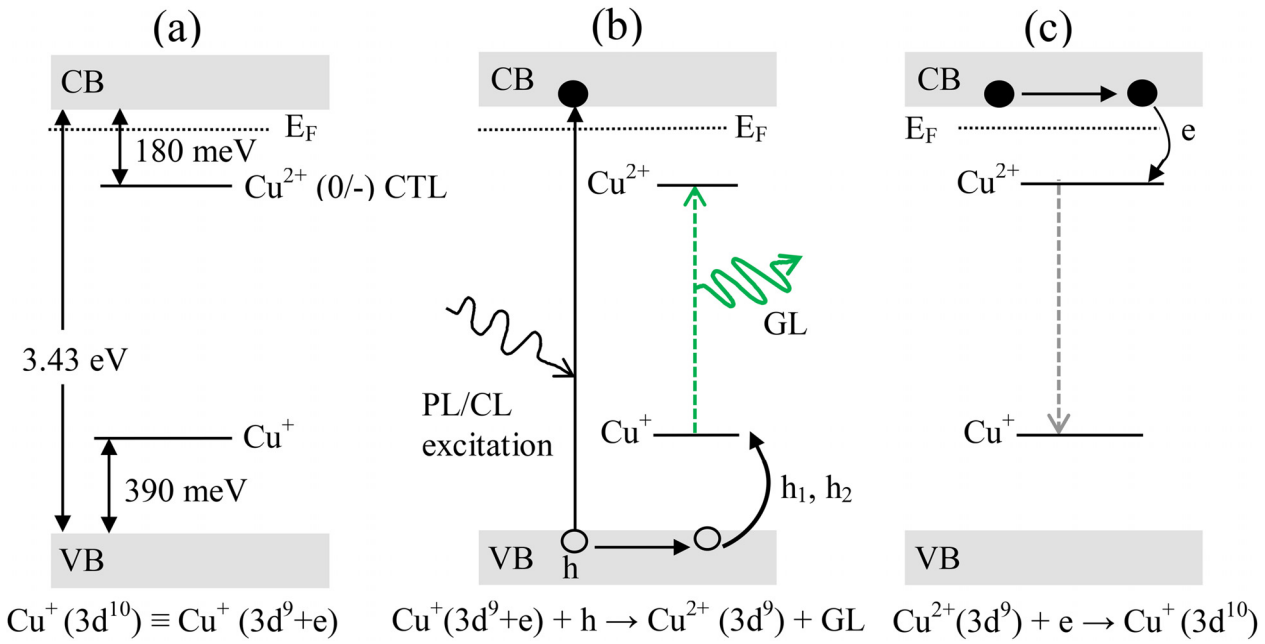

FIG. 4. Schematic energy level diagram to illustrate the transitions involved between the Cu ground and excited states in Ga-doped ZnO nanorods. (a) Cu is in the Cu^+ ($3d^{10}$) state as the Fermi level is raised above the (0/-) CTL of Cu centers via the Ga donor doping. (b) Holes are captured by $Cu^+(3d^9+e)$ placing it in an excited state, which emits GL and relaxes to the $Cu^{2+}(3d^9)$ ground state, and (c) Cu^{2+} captures a free electron from the CB returning it to the Cu^+ state.

fine structures in the green band. This luminescence band is attributed to hole transition to the negatively charged Cu^+ state located at 390 meV above the valence band.

See supplementary material for detailed characterization of the Ga-doped ZnO nanorods and Cu acceptors.

This work was supported under Australian Research Council (ARC) Discovery Project funding scheme (project number DP150103317) and partly undertaken on the Soft X-ray Spectroscopy beamline at the Australian Synchrotron, Australia. M. Azizar Rahman acknowledges the financial support of Australian Government through an International Postgraduate Research Scholarship (IPRS).

[1]J. Kim, G. V. Naik, A. V. Gavrilenko, K. Dondapati, V. I. Gavrilenko, S. M. Prokes, O. J. Glembocki, V. M. Shalaev, and A. Boltasseva, Phys. Rev. X **3**, 041037 (2013).
[2]K. S. Shin, K. H. Lee, H. H. Lee, D. Choi, and S. W. Kim, J. Phys. Chem. C **114**, 15782 (2010).
[3]B. K. Meyer, H. Alves, D. M. Hofmann, W. Kriegseis, D. Forster, F. Bertram, J. Christen, A. Hoffmann, M. Strassburg, M. Dworzak *et al.*, Phys. Status Solidi B: Basic Res. **241**, 231 (2004).
[4]K. Johnston, M. O. Henry, D. McCabe, E. McGlynn, M. Dietrich, E. Alves, and M. Xia, Phys. Rev. B **73**, 165212 (2006).
[5]C. Ton-That, L. Weston, and M. R. Phillips, Phys. Rev. B **86**, 115205 (2012).
[6]R. Dingle, Phys. Rev. Lett. **23**, 579 (1969).
[7]N. Y. Garces, L. Wang, L. Bai, N. C. Giles, L. E. Halliburton, and G. Cantwell, Appl. Phys. Lett. **81**, 622 (2002).
[8]N. Kouklin, Adv. Mater. **20**, 2190 (2008).
[9]M. A. Reshchikov, V. Avrutin, N. Izyumskaya, R. Shimada, H. Morkoc, and S. W. Novak, J. Vac. Sci. Technol. B **27**, 1749 (2009).
[10]C. W. Zhang, C. Han, S. S. Yan, and F. B. Zheng, Europhys. Lett. **95**, 47011 (2011).
[11]Z. A. Khan, A. Rai, S. R. Barman, and S. Ghosh, Appl. Phys. Lett. **102**, 022105 (2013).
[12]D. B. Buchholz, R. P. H. Chang, J. H. Song, and J. B. Ketterson, Appl. Phys. Lett. **87**, 082504 (2005).
[13]Q. Y. Xu, H. Schmidt, S. Q. Zhou, K. Potzger, M. Helm, H. Hochmuth, M. Lorenz, A. Setzer, P. Esquinazi, C. Meinecke *et al.*, Appl. Phys. Lett. **92**, 082508 (2008).
[14]C. Ton-That, M. Foley, and M. R. Phillips, Nanotechnology **19**, 415606 (2008).
[15]Z. Yang, D. C. Look, and J. L. Liu, Appl. Phys. Lett. **94**, 072101 (2009).
[16]J. Cizek, J. Valenta, P. Hruska, O. Melikhova, I. Prochazka, M. Novotny, and J. Bulir, Appl. Phys. Lett. **106**, 251902 (2016).
[17]Y. D. Liu, H. W. Liang, L. Xu, J. Z. Zhao, J. M. Bian, Y. Luo, Y. Liu, W. C. Li, G. G. Wu, and G. T. Du, J. Appl. Phys. **108**, 113507 (2010).
[18]B. Wei, K. Zheng, Y. Ji, Y. F. Zhang, Z. Zhang, and X. D. Han, Nano Lett. **12**, 4595 (2012).
[19]Y. Kanai, Jpn. J. Appl. Phys., Part 1 **30**, 703 (1991).
[20]D. C. Look, K. D. Leedy, L. Vines, B. G. Svensson, A. Zubiaga, F. Tuomisto, D. R. Doutt, and L. J. Brillson, Phys. Rev. B **84**, 115202 (2011).
[21]M. Grundmann, *The Physics of Semiconductors: An Introduction Including Nanophysics and Applications* (Springer, Berlin, Heidelberg, 2016), p. 189.
[22]R. Heinhold, G. T. Williams, S. P. Cooil, D. A. Evans, and M. W. Allen, Phys. Rev. B **88**, 235315 (2013).
[23]M. Oshikiri, Y. Imanaka, F. Aryasetiawan, and G. Kido, Phys. B **298**, 472 (2001).
[24]P. Dahan, V. Fleurov, P. Thurian, R. Heitz, A. Hoffmann, and I. Broser, J. Phys.: Condens. Matter. **10**, 2007 (1998).
[25]S. Mukamel, *Principles of Nonlinear Optical Spectroscopy* (Oxford University Press, New York, 1999), p. 227.
[26]R. Kuhnert and R. Helbig, J. Lumin. **26**, 203 (1981).